Interferon-induced Transmembrane Protein 1 restricts replication of virus that enter cells via the plasma membrane.

S. E. Smith[†1,6], D. C. Busse[†2], Š. Binter[1,6], S. Weston[3], C. Diaz Soria[1], B. M. Laksono[4], S. Clare[1], S. Van Nieuwkoop[4], B. G. Van den Hoogen[4], M. Clement[5], M. Marsden[5], I. R. Humphreys[5], M. Marsh[4], R. L. de Swart[3], R. S. Wash[1,6], J. S. Tregoning[*2], P. Kellam[*1,2,6]

[1]Wellcome Trust Sanger Institute, Wellcome Trust Genome Campus, Hinxton, CB10 1SA, United Kingdom

[2]Mucosal Infection & Immunity Group, Section of Virology, Imperial College London, St. Mary's Campus, London, W2 1PG, United Kingdom

[3]Department of Viroscience, Erasmus MC, 3015 CE Rotterdam, The Netherlands

[4]MRC Laboratory for Molecular Cell Biology, University College London, Gower Street, London, WC1E 6BT, United Kingdom

[5]Division of Infection and Immunity/Systems Immunity University Research Institute, Cardiff University, Cardiff, CF14 4XN, United Kingdom

[6]Kymab Ltd, The Bennet Building (B930), Babraham Research Campus, Cambridge CB22 3AT, United Kingdom.

[†]These authors contributed equally to the work.

*Contact information for corresponding authors: paul.kellam@imperial.ac.uk and john.tregoning@imperial.ac.uk

Key words: IFITM1, restriction factor, innate immunity, paramyxovirus

Word count text:
Word count abstract: 233

Abstract:

The acute anti-viral response is mediated by a family of interferon stimulated genes (ISG), providing cell-intrinsic immunity. Mutations in genes encoding these proteins are often associated with increased susceptibility to viral infections. One family of ISGs with anti-viral function are the interferon-inducible transmembrane proteins (IFITM) of which IFITM3 has been studied extensively. By contrast, IFITM1 has not been studied in detail. Since IFITM1 can localise to the plasma membrane, we investigated its function with a range of enveloped viruses thought to infect cells by fusion with the plasma membrane. Overexpression of IFITM1 prevented infection by a number of *Paramyxoviridae* and *Pneumoviridae*, including Respiratory Syncytial Virus (RSV), mumps virus and human metapneumovirus (HMPV). IFITM1 also restricted infection with an enveloped DNA virus that can enter via the plasma membrane, herpes simplex virus 1 (HSV-1). To test the importance of plasma membrane localisation for IFITM1 function, we identified blocks of amino acids in the conserved intracellular loop (CIL) domain that altered the subcellular localisation of the protein and reduced anti-viral activity. Screening published datasets, twelve rare non-synonymous SNPs were identified in human *IFITM1*, some of which are in the CIL domain. Using an *Ifitm1*$^{-/-}$ knock-out mouse we show that RSV infection was more severe, thereby extending the range of viruses restricted *in vivo* by IFITM proteins and suggesting overall that IFITM1 is broadly anti-viral and this anti-viral function is associated with cell surface localisation.

62 **Importance**

63 Host susceptibility to viral infection is multifactorial, but early control of viruses
64 not previously encountered is predominantly mediated by the interferon
65 stimulated gene (ISG) family. There are upwards of 300 of these genes, the
66 majority of which do not have a clearly defined function or mechanism of
67 action. The cellular location of these proteins may have an important effect on
68 their function. One ISG located at the plasma membrane is Interferon
69 inducible transmembrane protein 1 (IFITM1). Here we demonstrate that
70 IFITM1 can restrict a range of viruses that enter via the plasma membrane.
71 Mutant IFITM1 proteins that were unable to localise to the plasma membrane
72 did not restrict viral infection. We also observed for the first time that IFITM1
73 plays a role in vivo, *Ifitm1*$^{-/-}$ knock-out mice were more susceptible to viral lung
74 infection. This data contributes to our understanding of how ISG prevent viral
75 infections.
76

Introduction

Intrinsic immunity is the ability of infected and bystander cells to restrict infection prior to the recruitment of innate or adaptive immune cells (1). This intrinsic immune response is in part mediated by proteins encoded by interferon stimulated genes (ISG). There are over 300 of these genes that are upregulated in response to type I, II and III interferons (2). Although the functions and modes of action of a few of these genes have been studied in detail, many remain to be functionally characterised (3). Nevertheless, the importance of ISGs in defence against various pathogens is demonstrated by increased disease severity associated with single nucleotide polymorphisms (SNPs) in genes encoding ISGs including *IFITM3* (4), *MDA5* (5), *OAS-1* (6), and *Mx1* (6-8).

One family of ISGs that functions as broad-spectrum inhibitors of viral replication is the Interferon-inducible transmembrane protein (IFITM) family. IFITMs are functionally conserved across many species, including birds (9-12), pigs (13, 14), and bats (13). In most cases this family of restriction factors block infection during virus entry into cells (15), although additional mechanisms have been proposed (16, 17). It is proposed that these very similar proteins arose by gene duplication events (18), but their maintenance across many species suggests they have distinct functions or specialisations. While IFITM2 and IFITM3 share 90% of their amino acids, IFITM1 shares only 74% with IFITM3, due largely to an N-terminal deletion of 21 amino acids. Research into IFITM proteins has mainly focussed on IFITM3 and investigation of its ability to inhibit entry and replication of RNA viruses, including influenza (19-22), dengue virus (20, 23), Zika virus (24), RSV (25), Semliki Forest and Sindbis viruses (26) and murine cytomegalovirus (mCMV) (27). Fewer studies have been performed on IFITM1, which can restrict a number of RNA viruses, including hepatitis C virus (28, 29), Sheep Jaagsikie virus (30), HIV (31), Zika virus (24), and influenza viruses (20), but not Rift Valley fever virus (32), Sindbis or Semliki Forest virus (26). IFITM1 has no reported antiviral activity against the non-enveloped DNA viruses human papillomavirus and adenovirus (33).

Interestingly, the IFITM proteins differ in their sub-cellular localisation when expressed individually: IFITM1 is found primarily on the cell surface (10, 34), IFITM2 in late endosomes and IFITM3 mainly in early endosomes (34). The function of IFITM1 may thus be linked to its abundance in the plasma membrane. Indeed, mutations that increase IFITM1 cell surface expression lead to increased restriction of HIV-1_{NL4-3} infection compared to wildtype IFITM1 (31). Moreover, mutations in IFITM1 that prevent it binding to the vesicular transport adaptor protein AP3 reduced inhibition of viral replication (35).

Greater examination of the range of viruses restricted by IFITM1 and the effect of engineered and naturally occurring mutations in IFITM1 is required to further understand the mechanism of IFITM1 viral restriction. Here we show that *in vitro* IFITM1 inhibits infection of several RNA viruses that enter via the plasma membrane, including mumps virus, Respiratory Syncytial Virus (RSV), human metapneumovirus (HMPV), and a DNA virus, herpes simplex virus 1 (HSV-1). Further, we show that otherwise healthy *Ifitm1*$^{-/-}$ knock-out mice experience more severe RSV infection compared to wild type mice. However, mCMV infection, which is altered in *Ifitm3*$^{-/-}$, mice was no more severe in *Ifitm1*$^{-/-}$ knock-out mice. This suggests that IFITM1 has anti-viral activity that is distinct to IFITM3.

Methods:

Cell culture. A549 cells (ATCC: CCL-185) were grown in F-12 media (Life Technologies), MRC-5 (ATCC: CCL-171) were grown in EMEM (ATCC), U2OS cells (ATCC: HTB-96) were grown in McCoy's media (Life Technologies). Vero cells (Sigma: 84113001), HEp2 cells (ATCC: CCL-23) and HEK293-T/17 cells (ATCC: CRL-11268) were grown in DMEM (Life Technologies). All media were supplemented with 10 % v/v FBS (Biosera).

Overexpression studies. Human IFITM1 wildtype and alanine-scanned gene sequences were synthesised (GeneArt, Life Technologies) for expression in human cells. Single amino acid changes were introduced using site-directed mutagenesis (Quikchange II XL, Agilent). All IFITM genes were cloned into the *BamH*I and *Not*I sites of the lentivirus vector, pSIN-BN_puro (36), and sequences confirmed by capillary sequencing (GATC Biotech). The wildtype human genes cloned were IFITM1 (MK288009), IFITM2 (MK288010) and IFITM3 (MK288011). The gene cassette was cloned into pSIN-BN along with a C-terminal HA tag to facilitate analysis of the expressed protein. Lentivirus vector stocks were made by a three-plasmid transfection of HEK293-T/17 cells, grown to confluence in a 10 cm^2 dish (10). The lentiviruses were used to transduce A549 or Vero cells and produced a mixed population of IFITM expressing cells. Transduced cells were selected using puromycin (concentrations of 1.4 µg/ml and 5.2 µg/ml, respectively). Expression of IFITM proteins was detected by western blotting using an antibody against the HA tag (ab18181, Abcam), IFITM1 (HPA004810, Sigma) or IFITM3 (AP1153a, Abgent).

IFITM1 Localisation. The localisation of IFITM-HA-tagged proteins was assessed using an anti-HA antibody conjugated to Dylight-550 (ab117502, Abcam). Coverslips were washed in PBS and adhered to microscopy slides using ProLong Gold with DAPI (ThermoFisher). Cells were imaged using microscopy after permeabilisation in 0.25% triton X and fixed in 4% paraformaldehyde, images were taken at 63X objective. Expression of the HA tagged IFITM1 on non-fixed and non-permabilised cells was quantified by flow cytometry using an anti-HA antibody conjugated to Alexa Fluor 647 (682404, Biolegend). Cells were washed in PBS and harvested by trypsinisation. Cells

were washed in 3% FBS PBS and stained with antibody. Analysis was performed on an LSR Fortessa flow cytometer (BD Biosciences).

RNA virus *in vitro* infections. Transduced Vero cells were seeded at $2x10^5$ cells per well in 24-well plates. The following day cells were infected with different paramyxoviruses: parainfluenza virus rgPIV3 (MOI 0.1) (37); measles virus (MV), rMV^{rEdt}EGFP (MOI (38) and rMV^{EZ}EGFP (39); mumps virus (unpublished Rennick *et al*.); Newcastle disease virus NDV, rNDV-GFP-F0 (40), the orthomyxovirus influenza A virus PR/8/1934-EGFP (MOI 1) (41); and pneumoviruses Respiratory Syncytial Virus B strain rHRSV^{B05}EGFP (42) and strain A2 rgRSV (43); human metapneumovirus HMPV NL/1/00-GFP (44), and HMPV NL/1/99-GFP (45). After 24 hr, cells were fixed in 2 % v/v paraformaldehyde (PFA) and the percentage of infected cells was measured by detecting GFP expression using flow cytometry.

HSV-1 *in vitro* infections.

HSV-1 C12, a variant that has a CMV IE1 promoter–EGFP cassette inserted at the US5 gene locus from pEGFP-C1 (Clontech), a kind gift from Dr Stacey Efstathiou, was used for these experiments (46). Virus stocks were propagated and titrated on confluent BHK-21 cells.

HSV-1/GFP infection, at MOI 5 for A549 and MOI 0.5 for MRC-5, was determined by fluorescence microscopy at 7 hours post infection (hpi) unless stated otherwise, following fixation with 4 % v/v PFA for 20 min and permeabilisation using 0.3 % v/v TritonX / PBS (10 min). Cells were washed with 100 µl of PBS / Hoechst solution (Life Technologies, 200 ng/µl). The fixed cells were analysed to determine the proportion of cells expressing GFP (Cellomics ArrayScan VTI, Thermofisher), using the Target Activation bioapplication. Briefly, this method counts every cell on the plate by drawing a perimeter around each nuclei (detected by Hoechst) and calculates the percentage of these cells expressing GFP. Alternatively, flow cytometry was used to quantify HSV-1/GFP infection. Cells were washed in PBS and removed from the plastic using trypsin. Cells were washed again in PBS and fixed in 4 % v/v PFA for 10 min at RT. Cells were washed and resuspended in

PBS and analysed for GFP expression using a FACS Calibur (Becton Dickinson).

Knock-down of IFITM1 using siRNA treatment. MRC-5 cells were seeded in triplicate in 12-well plates at $6x10^4$ per well. The following day cells were either treated with 5 µl of PBS (mock), 5 µl of IFNα2a (PBL Interferon), 5 µM of human IFITM1 SMARTpool siRNA (L-019543-00, Dharmacon), or 5 µM of non-targeting pool siRNA (NT siRNA (D-001810-10, Dharmacon)). Transfections were carried out using the Dharmafect reagent according to the manufacturer's guidelines.

Confirmation of protein expressing using western blot. Total protein was quantified by BCA assay (Thermo Scientific) and equal amounts of protein were loaded onto Mini-PROTEAN® TGX™ precast SDS-PAGE gels (Biorad). Proteins were transferred onto nitrocellulose membranes using a TransBlot Turbo apparatus (Bio-Rad). Nitrocellulose membranes were blocked overnight using 5 % w/v milk powder/PBS-Tween. Proteins were visualised with the following primary antibodies: human IFITM3 (rabbit anti-IFITM3 [N-terminal amino acids 8–38; AP1153a, Abgent]); human IFITM1 (rabbit anti-IFITM1 [HPA004810, Sigma]); β actin (rabbit anti- β actin [ab8227, Abcam]) was used as a loading control. All primary antibodies were visualised using species-specific horseradish peroxidase-conjugated secondary antibodies (Dako).

Bioinformatic analysis. Custom scripts (available on request) were used to extract single variants in the IFITM1 locus of people in the 1000Genomes phase3 cohort and people recruited in the following UK10K cohorts: UK10K_Neuro_Aberdeen, UK10K_Neuro_Asd-_Gallagher, UK10K_Neuro _Edinburgh, UK10K_Neuro_Gurling, UK10K_-Neuro_Iop_Collier, UK10K_ Neuro_Muir, UK10K_Obesity_Gs, UK10K_-Obesity_Twinsuk, UK10K_Rare _Hyperchol, UK10K_Rare_Neuromuscular, UK10K_Rare_Sir, UK10K_ TwinsUK, UK10K_ALSPAC. Resulting SNPs were analysed using the Variant Effect Predictor tool (Ensembl) displaying results as one consequence per variant. Visualisation of SNP was performed using Protter (47).

Mice husbandry and phenotyping. Background-matched 8-10 week old wild type or *Ifitm1*$^{-/-}$ (Wellcome Trust Sanger Institute) (48), all of which were

>95 % C57BL/6, were supplied with food and water *ad libitum* and were monitored daily for signs of illness. *Ifitm1*$^{-/-}$ gene knockout (KO) mice were phenotyped through pipelines at the Wellcome Trust Sanger Institute, as described previously (49, 50). To investigate IFITM1 gene expression BALB/c 8-10 week old mice were obtained from Charles River (Bath, UK) and housed at the central biomedical sciences at Imperial College London. All animal experiments were maintained in accordance with UK Home Office regulations, UK Animals (Scientific Procedures) Act 1986 and reviewed by the Wellcome Trust Sanger Institute's or Imperial College London's Animal Welfare and Ethical Review Boards.

RSV *in vivo* infection. RSV strain A2 (kind gift from Prof P. Openshaw, Imperial College London) was grown in HEp-2 cells and viral titres determined by plaque assay. Mice were infected intranasally with 5x10^5 plaque forming units (PFU) under isoflurane anaesthesia. Weight was measured daily to monitor disease severity. At day 7 after infection, lungs were removed, the smaller lobe was snap frozen in liquid nitrogen for RNA extraction and the remainder was homogenised by passage through 100 µm cell strainers (Falcon). RSV viral load was measured by quantitative RT-PCR for the RSV L gene using primers and probes previously described (51), with copy number determined using a curve and presented relative to µg lung RNA. Lungs were homogenised with a rotor-stator homogeniser, centrifuged and the supernatant collected for cytokine analyses. Cytokines in lung homogenates were quantified by ELISA using duosets from R&D Systems.

mCMV infections. Smith strain mCMV was propagated *in vivo*, and virus stock and viral load in tissues of infected mice quantified by plaque assay, as previously described (27). Mice were infected with 3x10^4 PFU of virus via the intra-peritoneal route. IL-6 in organ homogenate was quantified using ELISA (Biolegend). For *in vitro* infections, MEFs and bone marrow-derived myeloid cells were infected with mCMV and virus production quantified as previously described (27).

Results

Restriction of Paramyxoviridae and Pneumoviridae by human IFITM1

Previous studies have demonstrated that IFITM1 can restrict infection by some RNA viruses (20, 24, 28, 29, 31). Given our previous findings, that IFITM1 is preferentially localised to the cell surface (34), we sought to extend these findings to the *Paramyxoviridae* and *Pneumoviridae*, which are negative-stranded RNA viruses that are thought to enter cells at the plasma membrane. These families include viruses of clinical importance such as measles (MV), mumps virus and RSV. Lentiviral vectors were used to stably over-express IFITM1, 2 or 3 proteins in Vero cells, which are permissive to infection with the described viruses. The proteins were HA-tagged to enable detection and transfection led to detectable expression in the cells (Fig 1A). IFITM1 expression in Vero cells was observed throughout the cell, with a concentration in the perinuclear space and, unlike IFITM2 and IFITM3 which were localised internally and form a punctate pattern, distinct expression at the cell surface (Fig 1B). Cell surface expression of IFITM1 was confirmed by flow cytometry analysis on non-fixed and non-permeabilised cells (Fig 1C) and co-localisation with wheat germ agglutinin (Fig 1D). . This pattern of expression was consistent with previous studies which further confirmed cell surface expression of IFITM1 in these cell lines using additional assays (34).

IFITM1-3 transduced Vero cells were infected with different members of the *Paramyxoviridae* and *Pneumoviridae* and infection compared to Vero cells transduced with an empty vector. IFITM1 restricted infection of all the viruses tested, including parainfluenza virus (PIV), RSV, human metapneumovirus (hMPV), Newcastle disease virus (NDV) and mumps virus (Fig 1E). There was a small, but significant, effect on measles virus and NDV replication. IFITM2 had no impact on any of the viruses tested. As shown previously, only RSV was restricted by IFITM3 (25, 52). Comparisons were made to influenza virus (an orthomyxovirus) which confirmed both IFITM1 and IFITM3 are able to restrict influenza A effectively.

IFITM1 restricts HSV-1 infection

These data support an anti-viral role for IFITM1 against a selected group of RNA viruses. Previous studies have suggested that IFITM1 has no significant impact on DNA viruses such as papilloma and adenoviruses. However, both of these are non-enveloped viruses which, for the most part, are not restricted by IFITM proteins. To explore the role of IFITM1 on enveloped DNA viruses that can enter the cell via the plasma membrane, we looked at the effect of IFITM1 expression on infection by Herpes Simplex virus (HSV-1), a member of the Alphaherpesvirinae. A549 human fibroblasts were transduced with lentiviruses coding for human IFITM1, IFITM2 or IFITM3 proteins. Transfected cells were infected with HSV-1/GFP virus at a multiplicity of infection (MOI) of 5. Quantitative fluorescence microscopy showed that at 7 hpi 16 % of cells expressing IFITM1 were infected by HSV-1 compared to 87 % and 107 % of cells expressing IFITM3 and IFITM2, respectively (values normalised to un-transduced cells) (Fig 2A). These findings were supported by flow cytometry analysis of a multi-cycle HSV-1 infection. After 44 hr, HSV infection (MOI 0.01) in IFITM1 expressing A549s was 36.6 % compared to 75.5% and 58.1% for IFITM2 and IFITM3, respectively, and 75.1% infection of control empty vector transduced cells (Fig 2B).

To confirm the role of IFITM1, we looked at the effect of gene knockdown. A SMARTpool of siRNAs targeting human IFITM1 reduced expression of IFITM1 mRNA in MRC-5 cells by 96 % (-4.72$\log_2$ reduction) compared to Interferon alpha treatment (Fig 2C). The non-targeting control had some effect on IFITM1 transcription. Pre-treatment with the human IFITM1 specific siRNAs increased HSV-1 infection, compared to untreated cells and a non-targeting siRNA control (Fig 2D). Pre-treatment with IFNα2a substantially reduced HSV-1 infection, but the addition of siRNA against IFITM1 to IFNα2 treated cells negated the effect of the IFNα2a. Collectively, these data suggest that IFITM1 is an important part of the IFN response to HSV-1 infection.

Amino acids in the CIL domain of IFITM1 are important for restriction

The current model of IFITM1 structure establishes it as having its short N-terminal domain in the cytoplasm, two membrane domains linked by a conserved intracellular loop (CIL) exposed to the cytoplasm and the C-

terminal domain exposed on the cell surface (34). In order to determine the amino acids that are important for IFITM1 localisation and virus restriction, we generated a panel of 20 cell lines expressing mutant proteins with consecutive substitutions of six alanines, starting from the second N-terminal amino acid (Fig 3A). These mutated proteins were expressed in A549 cells (Fig 3B) and their localisations established by immunofluorescence using an antibody against the C-terminal HA-tag (Fig 3C). Since the CIL domain is predicted to be exposed to the cytoplasm (34), mutations in this domain were not expected to alter IFITM1 localisation. However, in the 6-alanine mutants AA-63, 69 and 83 IFITM1 was not seen at the cell surface but was primarily associated with LAMP1-negative (a marker for late endosomes and lysosomes) intracellular membranes. Interestingly, AA-76 IFITM1 appeared to show both intracellular and surface localisation. The loss of cell surface expression with mutation of the CIL domain was confirmed by flow cytometry on non-fixed and non-permeabilsed cells, wild type protein was detected at significantly higher levels on the cell surface than the AA-63, 69 or 83 mutants (Fig 3D, E), there was no significant difference in surface expression of the AA-76 mutant and the wildtype. However, there was a decrease in the median fluorescence intensity (MFI) of A549 AA-76 cells suggesting that there is reduced levels of cell surface IFITM1 expression (Fig 3.E).

To determine whether mutations in the CIL domain affected function, cells expressing wildtype IFITM1, a negative control Empty vector, or IFITM1 with 6-alanines inserted at AA-63, 69, 76 or 83 were infected with influenza, measles virus, mumps virus, or RSV. As observed previously, overexpression of wild type IFITM1 reduced infection for all tested viruses, relative to empty cells (Fig 3F, 3G). Cell lines expressing IFITM1 AA-63, 69, 76, or 83 mutants showed increased infection relative to cells expressing the wild type IFITM1, suggesting an impairment of IFITM-mediated restriction. Interestingly IFITM1 AA-76, which was seen to maintain some cell surface expression unlike the other mutant proteins, was still able to restrict RSV ~20% (Fig 3G). However, this was still a significant reduction in restriction compared to that observed with over-expression of the wild type protein. Together, the infectivity and immunofluorescence data indicate that the CIL domain influences IFITM1

localisation and is important for IFITM1's anti-viral activity. This may suggest that IFITM1 function is dependent upon its localisation to the cell surface, rather than intracellular membranes, which requires an intact CIL domain.

Having observed that IFITM1 can restrict infection by enveloped RNA and DNA viruses and that sequence alterations in the CIL domain effectively impair function, we investigated whether there are common SNPs in the IFITM1 gene. To map these SNPs, variants were identified in *IFITM1* from the 1000Genomes phase 3 dataset (2504 people), the UK10K control cohorts (2453 people) and 11 UK10K disease cohorts (6053 people). In total, 93 SNPs were identified across the entire gene (Fig 3H). Of these 12 (20 %) resulted in non-synonymous substitutions, but all SNPs were very rare and were rarely seen in multiple cohorts (Table 1). The exception is SNP rs9667990 (P13A), which is seen in the vast majority of individuals; it is likely therefore that a proline at AA13 was a rare amino acid substitution in the reference sequence and that alanine is the correct, common amino acid. The location of these non-synonymous SNPs is shown across the whole of the IFITM1 protein (Fig 3I).

RSV disease is more severe in mice lacking IFITM1

As IFITM1 affects viral replication *in vitro*, we wished to determine its role *in vivo*. *Ifitm1*$^{-/-}$ mice and wild type C57BL/6 mice were intranasally infected with RSV A2, and were monitored daily for weight loss for seven days after infection (Fig 4A). *Ifitm1*$^{-/-}$ mice showed significant weight loss on day seven after infection compared to wild type littermates ($p<0.05$) (Fig 4A). There was significantly higher lung RSV viral load at day four after infection (Fig 4B), and significantly more cells in the airways at day 4 (Fig 4C) and lungs at day 7 (Fig 4D) after infection. To determine the effect of IFITM1 on the inflammatory response, the lungs of all mice were homogenised and the levels of IL-6 (Fig 4E) and IL-1β (Fig 4F) compared between genotypes after RSV infection. The levels of both cytokines were significantly higher in infected KO mice compared to wildtype littermates.

To test the effect of IFITM1 in an established herpesvirus model, we infected WT and *Ifitm1*$^{-/-}$ mice with the beta herpesvirus murine CMV (mCMV). IFITM1 deficiency did not impact virus-induced weight loss in this model (Fig 4G). Moreover, in accordance with the reported lack of role for IFITM1 in restriction of hCMV replication (33, 53), mCMV replication was not increased in the absence of IFITM1 *in vivo* (Fig 4H). Given that IFITM1 deficiency during RSV infection led to an increased IL-6 production and *Ifitm3*$^{-/-}$ mice suffer from IL-6 driven pathogenesis during mCMV infection (27), we assessed IL-6 production in mCMV-infected *Ifitm1*$^{-/-}$ mice. In accordance with unaltered weight loss observed in these mice, Ifitm1 deficiency did not influence virus-induced cytokine production (Fig 4I). As mCMV and RSV infect different tissues we quantified basal *Ifitm1* expression in the lungs, liver, and spleens of wild-type BALB/c mice (Fig 4.L). Expression was detectable in each tissue but was significantly lower in the liver. However, expression was comparable between lung and spleen tissue. Further, when BMDMs and MEFs from wild-type and KO mice were infected *ex vivo* with mCMV there was no difference in viral titres (Fig 4J, 4K).Thus, overall, these data demonstrate that IFITM1 does not influence the replication and associated pathogenesis of a beta-herpesvirus *in vivo*.

Discussion

Here we demonstrate that IFITM1 has wide ranging anti-viral function, restricting the replication of RNA viruses from the *Paramyxoviridae* and *Pneumoviridae*. Importantly, for the first time we demonstrate anti-viral function of IFITM1 against a DNA virus, HSV-1. Our findings suggest that the cellular localisation of the protein is critical for its function.

Sequential mutation of the CIL domain of IFITM1 revealed that this domain was essential in determining cellular localisation and antiviral activity. Stably-transduced Vero cells were found to express wild type IFITM1 in a diffuse manner likely on the cell surface, but also potentially in the cytoplasm. Previous studies, including the initial study identifying IFITM1 (referred to as surface antigen Leu-13 antigen and subsequently CD225) have shown that IFITM1 is primarily expressed on the plasma membrane (54). Most

subsequent studies have shown that IFITM1 has domains expressed on the cell surface using a range of assays including cell-surface biotinylation and antibody labelling in the absence of plasma membrane disruption (10, 28, 34, 55). However, some studies have suggested that IFITM1 is also expressed internally in vesicles distinct from either IFITM2 or 3, although they have not been specifically identified (32, 35). Here we find evidence for different cellular locations of IFITM1 with mutation of the CIL domain: interestingly the AA-76 mutant showed the highest level of cell surface expression and the greatest reduction of RSV infection. A proposed mechanism of action for the IFITM proteins is that they alter the fluidity of cellular membranes preventing fusion with the infecting virus envelope (21, 30). We suggest that IFITM1, unlike IFITM2 and IFITM3, primarily functions through alteration of the plasma membrane and as such is able to restrict viruses at this initial point in infection.

This is the first reported study describing viral infection in *Ifitm1*$^{-/-}$ animals. Uninfected *Ifitm1*$^{-/-}$ mice were phenotypically normal as assessed by the Wellcome Trust Sanger Institute murine phenotyping pipelines. We observed a different phenotype depending on the virus infection, *Ifitm1*$^{-/-}$ mice were more susceptible to RSV infection as judge by viral RNA, cell infiltration, cytokine production and body weight loss. However, no effect was seen in mCMV-infected animals. This may in part be due to differences in where the infection is localised as there are lower levels of *Ifitm1* in the liver than in the lung. However, mCMV also establishes infection in the spleen after systemic administration (56) where there is comparable *Ifitm1* expression. It has been previously shown that another member of the IFITM family, IFITM3, restricts RSV *in vivo* (25). Interestingly IFITM3 has also been shown to restrict mCMV pathogenesis *in vivo*, and this is due to modulation of pro-inflammatory cytokine production rather than direct control of virus replication (27). The observation that IFITM1 did not influence mCMV pathogenesis in our experiments highlights fundamental functional differences between IFITM1 and IFITM3. Further studies of the immune-regulatory functions of IFITM3 and, possibly, IFITM1 will be informative.

Not all enveloped viruses are restricted by IFITM1. The differences in virus inhibition may reflect differences in the route by which the virus infects the cell, some viruses may bypass IFITM1 at the plasma membrane, for example mCMV enters certain cell types (e.g. myeloid cells) by endocytosis-dependent mechanisms (27). Furthermore, we cannot preclude the possibility that IFITM1 may restrict initial mCMV cell entry into other cells (e.g. fibroblasts) but that a subsequent previously described pro-viral role for IFITM1 (53) may mask this effect in our assays.

Further investigation into how IFITM1 affects human susceptibility to viral infection is required. We have previously reported that a SNP in IFITM3 were associated with more severe influenza infection (4). In the current study we report a list of SNPs found in the *IFITM1* gene. In the 11,000 individuals screened we identified 93 SNPs of which 20% were rare non-synonymous. Future studies will need to focus on how the protein interacts with viruses to prevent their entry into the cell. Improved understanding of the function of this ISG in the control of viral lung infection could also inform the design of novel anti-viral strategies.

Acknowledgements:

We thank Stephanie Czieso for assistance with fluorescence imaging. MM and SW were supported by UK Medical Research Council core funding to the MRC-UCL LMCB University Unit (grant numbers MC_UU12018/1 and MC_U12266B). DB was supported by The Wellcome Trust (109056/Z/15/A). IH is also funded by the Wellcome trust (207503/Z/17/Z).

References:

1. **Yan N, Chen ZJ.** 2012. Intrinsic antiviral immunity. Nat Immunol **13:**214-222.
2. **Schneider WM, Chevillotte MD, Rice CM.** 2014. Interferon-stimulated genes: a complex web of host defenses. Annu Rev Immunol **32:**513-545.
3. **McDonald JU, Kaforou M, Clare S, Hale C, Ivanova M, Huntley D, Dorner M, Wright VJ, Levin M, Martinon-Torres F, Herberg JA, Tregoning JS.** 2016. A Simple Screening Approach To Prioritize Genes for Functional Analysis Identifies a Role for Interferon Regulatory Factor 7 in the Control of Respiratory Syncytial Virus Disease. mSystems **1**.
4. **Everitt AR, Clare S, Pertel T, John SP, Wash RS, Smith SE, Chin CR, Feeley EM, Sims JS, Adams DJ, Wise HM, Kane L, Goulding D, Digard P, Anttila V, Baillie JK, Walsh TS, Hume DA, Palotie A, Xue Y, Colonna V, Tyler-Smith C, Dunning J, Gordon SB, Gen II, Investigators M, Smyth RL, Openshaw PJ, Dougan G, Brass AL, Kellam P.** 2012. IFITM3 restricts the morbidity and mortality associated with influenza. Nature **484:**519-523.
5. **Lamborn IT, Jing H, Zhang Y, Drutman SB, Abbott JK, Munir S, Bade S, Murdock HM, Santos CP, Brock LG, Masutani E, Fordjour EY, McElwee JJ, Hughes JD, Nichols DP, Belkadi A, Oler AJ, Happel CS, Matthews HF, Abel L, Collins PL, Subbarao K, Gelfand EW, Ciancanelli MJ, Casanova JL, Su HC.** 2017. Recurrent rhinovirus infections in a child with inherited MDA5 deficiency. J Exp Med **214:**1949-1972.
6. **Hamano E, Hijikata M, Itoyama S, Quy T, Phi NC, Long HT, Ha LD, Ban VV, Matsushita I, Yanai H, Kirikae F, Kirikae T, Kuratsuji T, Sasazuki T, Keicho N.** 2005. Polymorphisms of interferon-inducible genes OAS-1 and MxA associated with SARS in the Vietnamese population. Biochem Biophys Res Commun **329:**1234-1239.
7. **Ciencewicki JM, Wang X, Marzec J, Serra ME, Bell DA, Polack FP, Kleeberger SR.** 2014. A genetic model of differential susceptibility to human respiratory syncytial virus (RSV) infection. FASEB J **28:**1947-1956.
8. **Zhang X, Xu H, Chen X, Li X, Wang X, Ding S, Zhang R, Liu L, He C, Zhuang L, Li H, Zhang P, Yang H, Li T, Liu W, Cao W.** 2014. Association of functional polymorphisms in the MxA gene with susceptibility to enterovirus 71 infection. Hum Genet **133:**187-197.
9. **Smith J, Smith N, Yu L, Paton IR, Gutowska MW, Forrest HL, Danner AF, Seiler JP, Digard P, Webster RG, Burt DW.** 2015. A comparative

analysis of host responses to avian influenza infection in ducks and chickens highlights a role for the interferon-induced transmembrane proteins in viral resistance. BMC Genomics **16:**574.

10. **Smith SE, Gibson MS, Wash RS, Ferrara F, Wright E, Temperton N, Kellam P, Fife M.** 2013. Chicken interferon-inducible transmembrane protein 3 restricts influenza viruses and lyssaviruses in vitro. J Virol **87:**12957-12966.
11. **Blyth GA, Chan WF, Webster RG, Magor KE.** 2015. Duck Interferon-Inducible Transmembrane Protein 3 Mediates Restriction of Influenza Viruses. J Virol **90:**103-116.
12. **Bassano I, Ong SH, Lawless N, Whitehead T, Fife M, Kellam P.** 2017. Accurate characterization of the IFITM locus using MiSeq and PacBio sequencing shows genetic variation in Galliformes. Bmc Genomics **18**.
13. **Benfield CT, Smith SE, Wright E, Wash RS, Ferrara F, Temperton NJ, Kellam P.** 2015. Bat and pig IFN-induced transmembrane protein 3 restrict cell entry by influenza virus and lyssaviruses. J Gen Virol **96:**991-1005.
14. **Miller LC, Jiang Z, Sang Y, Harhay GP, Lager KM.** 2014. Evolutionary characterization of pig interferon-inducible transmembrane gene family and member expression dynamics in tracheobronchial lymph nodes of pigs infected with swine respiratory disease viruses. Vet Immunol Immunopathol **159:**180-191.
15. **Bailey CC, Zhong G, Huang IC, Farzan M.** 2014. IFITM-Family Proteins: The Cell's First Line of Antiviral Defense. Annu Rev Virol **1:**261-283.
16. **Wakim LM, Smith J, Caminschi I, Lahoud MH, Villadangos JA.** 2015. Antibody-targeted vaccination to lung dendritic cells generates tissue-resident memory CD8 T cells that are highly protective against influenza virus infection. Mucosal Immunol **8:**1060-1071.
17. **Yu J, Li M, Wilkins J, Ding S, Swartz TH, Esposito AM, Zheng YM, Freed EO, Liang C, Chen BK, Liu SL.** 2015. IFITM Proteins Restrict HIV-1 Infection by Antagonizing the Envelope Glycoprotein. Cell Rep **13:**145-156.
18. **Siegrist F, Ebeling M, Certa U.** 2009. Phylogenetic analysis of interferon inducible transmembrane gene family and functional aspects of IFITM3. Cytokine **48:**87-87.
19. **Bailey CC, Huang IC, Kam C, Farzan M.** 2012. Ifitm3 limits the severity of acute influenza in mice. PLoS Pathog **8:**e1002909.
20. **Brass AL, Huang IC, Benita Y, John SP, Krishnan MN, Feeley EM, Ryan BJ, Weyer JL, van der Weyden L, Fikrig E, Adams DJ, Xavier RJ, Farzan M, Elledge SJ.** 2009. The IFITM proteins mediate cellular resistance to influenza A H1N1 virus, West Nile virus, and dengue virus. Cell **139:**1243-1254.
21. **Desai TM, Marin M, Chin CR, Savidis G, Brass AL, Melikyan GB.** 2014. IFITM3 restricts influenza A virus entry by blocking the formation of fusion pores following virus-endosome hemifusion. PLoS Pathog **10:**e1004048.
22. **Feeley EM, Sims JS, John SP, Chin CR, Pertel T, Chen LM, Gaiha GD, Ryan BJ, Donis RO, Elledge SJ, Brass AL.** 2011. IFITM3 inhibits influenza A virus infection by preventing cytosolic entry. PLoS Pathog **7:**e1002337.

23. **Jiang D, Weidner JM, Qing M, Pan XB, Guo HT, Xu CX, Zhang XC, Birk A, Chang JH, Shi PY, Block TM, Guo JT.** 2010. Identification of Five Interferon-Induced Cellular Proteins That Inhibit West Nile Virus and Dengue Virus Infections. Journal of Virology **84:**8332-8341.
24. **Savidis G, Perreira JM, Portmann JM, Meraner P, Guo Z, Green S, Brass AL.** 2016. The IFITMs Inhibit Zika Virus Replication. Cell Rep **15:**2323-2330.
25. **Everitt AR, Clare S, McDonald JU, Kane L, Harcourt K, Ahras M, Lall A, Hale C, Rodgers A, Young DB, Haque A, Billker O, Tregoning JS, Dougan G, Kellam P.** 2013. Defining the Range of Pathogens Susceptible to Ifitm3 Restriction Using a Knockout Mouse Model. Plos One **8**.
26. **Weston S, Czieso S, White IJ, Smith SE, Wash RS, Diaz-Soria C, Kellam P, Marsh M.** 2016. Alphavirus Restriction by IFITM Proteins. Traffic **17:**997-1013.
27. **Stacey MA, Clare S, Clement M, Marsden M, Abdul-Karim J, Kane L, Harcourt K, Brandt C, Fielding CA, Smith SE, Wash RS, Brias SG, Stack G, Notley G, Cambridge EL, Isherwood C, Speak AO, Johnson Z, Ferlin W, Jones SA, Kellam P, Humphreys IR.** 2017. The antiviral restriction factor IFN-induced transmembrane protein 3 prevents cytokine-driven CMV pathogenesis. J Clin Invest **127:**1463-1474.
28. **Wilkins C, Woodward J, Lau DTY, Barnes A, Joyce M, McFarlane N, McKeating JA, Tyrrell DL, Gale M.** 2013. IFITM1 Is a Tight Junction Protein That Inhibits Hepatitis C Virus Entry. Hepatology **57:**461-469.
29. **Narayana SK, Helbig KJ, McCartney EM, Eyre NS, Bull RA, Eltahla A, Lloyd AR, Beard MR.** 2015. The Interferon-induced Transmembrane Proteins, IFITM1, IFITM2, and IFITM3 Inhibit Hepatitis C Virus Entry. J Biol Chem **290:**25946-25959.
30. **Li K, Markosyan RM, Zheng YM, Golfetto O, Bungart B, Li M, Ding S, He Y, Liang C, Lee JC, Gratton E, Cohen FS, Liu SL.** 2013. IFITM proteins restrict viral membrane hemifusion. PLoS Pathog **9:**e1003124.
31. **Jia R, Ding S, Pan Q, Liu SL, Qiao W, Liang C.** 2015. The C-terminal sequence of IFITM1 regulates its anti-HIV-1 activity. PLoS One **10:**e0118794.
32. **Mudhasani R, Tran JP, Retterer C, Radoshitzky SR, Kota KP, Altamura LA, Smith JM, Packard BZ, Kuhn JH, Costantino J, Garrison AR, Schmaljohn CS, Huang IC, Farzan M, Bavari S.** 2013. IFITM-2 and IFITM-3 but not IFITM-1 restrict Rift Valley fever virus. J Virol **87:**8451-8464.
33. **Warren CJ, Griffin LM, Little AS, Huang IC, Farzan M, Pyeon D.** 2014. The antiviral restriction factors IFITM1, 2 and 3 do not inhibit infection of human papillomavirus, cytomegalovirus and adenovirus. PLoS One **9:**e96579.
34. **Weston S, Czieso S, White IJ, Smith SE, Kellam P, Marsh M.** 2014. A membrane topology model for human interferon inducible transmembrane protein 1. PLoS One **9:**e104341.
35. **Li K, Jia R, Li M, Zheng YM, Miao C, Yao Y, Ji HL, Geng Y, Qiao W, Albritton LM, Liang C, Liu SL.** 2015. A sorting signal suppresses IFITM1 restriction of viral entry. J Biol Chem **290:**4248-4259.

36. **Zufferey R, Nagy D, Mandel RJ, Naldini L, Trono D.** 1997. Multiply attenuated lentiviral vector achieves efficient gene delivery in vivo. Nat Biotechnol **15:**871-875.

37. **Zhang L, Bukreyev A, Thompson CI, Watson B, Peeples ME, Collins PL, Pickles RJ.** 2005. Infection of ciliated cells by human parainfluenza virus type 3 in an in vitro model of human airway epithelium. J Virol **79:**1113-1124.

38. **de Vries RD, Lemon K, Ludlow M, McQuaid S, Yuksel S, van Amerongen G, Rennick LJ, Rima BK, Osterhaus AD, de Swart RL, Duprex WP.** 2010. In vivo tropism of attenuated and pathogenic measles virus expressing green fluorescent protein in macaques. J Virol **84:**4714-4724.

39. **Rennick LJ, de Vries RD, Carsillo TJ, Lemon K, van Amerongen G, Ludlow M, Nguyen DT, Yuksel S, Verburgh RJ, Haddock P, McQuaid S, Duprex WP, de Swart RL.** 2015. Live-attenuated measles virus vaccine targets dendritic cells and macrophages in muscle of nonhuman primates. J Virol **89:**2192-2200.

40. **Buijs P, van Nieuwkoop S, Vaes V, Fouchier R, van Eijck C, van den Hoogen B.** 2015. Recombinant Immunomodulating Lentogenic or Mesogenic Oncolytic Newcastle Disease Virus for Treatment of Pancreatic Adenocarcinoma. Viruses **7:**2980-2998.

41. **Spronken MI, Short KR, Herfst S, Bestebroer TM, Vaes VP, van der Hoeven B, Koster AJ, Kremers GJ, Scott DP, Gultyaev AP, Sorell EM, de Graaf M, Barcena M, Rimmelzwaan GF, Fouchier RA.** 2015. Optimisations and Challenges Involved in the Creation of Various Bioluminescent and Fluorescent Influenza A Virus Strains for In Vitro and In Vivo Applications. Plos One **10**.

42. **Lemon K, Nguyen DT, Ludlow M, Rennick LJ, Yuksel S, van Amerongen G, McQuaid S, Rima BK, de Swart RL, Duprex WP.** 2015. Recombinant Subgroup B Human Respiratory Syncytial Virus Expressing Enhanced Green Fluorescent Protein Efficiently Replicates in Primary Human Cells and Is Virulent in Cotton Rats. Journal of Virology **89:**2849-2856.

43. **Hallak LK, Collins PL, Knudson W, Peeples ME.** 2000. Iduronic acid-containing glycosaminoglycans on target cells are required for efficient respiratory syncytial virus infection. Virology **271:**264-275.

44. **Herfst S, de Graaf M, Schickli JH, Tang RS, Kaur J, Yang CF, Spaete RR, Haller AA, van den Hoogen BG, Osterhaus AD, Fouchier RA.** 2004. Recovery of human metapneumovirus genetic lineages a and B from cloned cDNA. J Virol **78:**8264-8270.

45. **de Graaf M, Herfst S, Schrauwen EJ, van den Hoogen BG, Osterhaus AD, Fouchier RA.** 2007. An improved plaque reduction virus neutralization assay for human metapneumovirus. J Virol Methods **143:**169-174.

46. **Arthur JL, Scarpini CG, Connor V, Lachmann RH, Tolkovsky AM, Efstathiou S.** 2001. Herpes simplex virus type 1 promoter activity during latency establishment, maintenance, and reactivation in primary dorsal root neurons in vitro. J Virol **75:**3885-3895.

47. **Omasits U, Ahrens CH, Muller S, Wollscheid B.** 2014. Protter: interactive protein feature visualization and integration with experimental proteomic data. Bioinformatics **30:**884-886.

48. **Lange UC, Adams DJ, Lee C, Barton S, Schneider R, Bradley A, Surani MA.** 2008. Normal germ line establishment in mice carrying a deletion of the Ifitm/Fragilis gene family cluster. Mol Cell Biol **28:**4688-4696.

49. **Ayadi A, Birling MC, Bottomley J, Bussell J, Fuchs H, Fray M, Gailus-Durner V, Greenaway S, Houghton R, Karp N, Leblanc S, Lengger C, Maier H, Mallon AM, Marschall S, Melvin D, Morgan H, Pavlovic G, Ryder E, Skarnes WC, Selloum M, Ramirez-Solis R, Sorg T, Teboul L, Vasseur L, Walling A, Weaver T, Wells S, White JK, Bradley A, Adams DJ, Steel KP, Hrabe de Angelis M, Brown SD, Herault Y.** 2012. Mouse large-scale phenotyping initiatives: overview of the European Mouse Disease Clinic (EUMODIC) and of the Wellcome Trust Sanger Institute Mouse Genetics Project. Mamm Genome **23:**600-610.

50. **White JK, Gerdin AK, Karp NA, Ryder E, Buljan M, Bussell JN, Salisbury J, Clare S, Ingham NJ, Podrini C, Houghton R, Estabel J, Bottomley JR, Melvin DG, Sunter D, Adams NC, Sanger Institute Mouse Genetics P, Tannahill D, Logan DW, Macarthur DG, Flint J, Mahajan VB, Tsang SH, Smyth I, Watt FM, Skarnes WC, Dougan G, Adams DJ, Ramirez-Solis R, Bradley A, Steel KP.** 2013. Genome-wide generation and systematic phenotyping of knockout mice reveals new roles for many genes. Cell **154:**452-464.

51. **Yamaguchi Y, Harker JA, Wang B, Openshaw PJ, Tregoning JS, Culley FJ.** 2012. Preexposure to CpG protects against the delayed effects of neonatal respiratory syncytial virus infection. J Virol **86:**10456-10461.

52. **Zhang W, Zhang L, Zan YL, Du N, Yang Y, Tien P.** 2015. Human respiratory syncytial virus infection is inhibited by IFN-induced transmembrane proteins. Journal of General Virology **96:**170-182.

53. **Xie M, Xuan B, Shan J, Pan D, Sun Y, Shan Z, Zhang J, Yu D, Li B, Qian Z.** 2015. Human cytomegalovirus exploits interferon-induced transmembrane proteins to facilitate morphogenesis of the virion assembly compartment. J Virol **89:**3049-3061.

54. **Deblandre GA, Marinx OP, Evans SS, Majjaj S, Leo O, Caput D, Huez GA, Wathelet MG.** 1995. Expression cloning of an interferon-inducible 17-kDa membrane protein implicated in the control of cell growth. J Biol Chem **270:**23860-23866.

55. **Amini-Bavil-Olyaee S, Choi YJ, Lee JH, Shi M, Huang IC, Farzan M, Jung JU.** 2013. The antiviral effector IFITM3 disrupts intracellular cholesterol homeostasis to block viral entry. Cell Host Microbe **13:**452-464.

56. **Hsu KM, Pratt JR, Akers WJ, Achilefu SI, Yokoyama WM.** 2009. Murine cytomegalovirus displays selective infection of cells within hours after systemic administration. Journal of General Virology **90:**33-43.

Figure Legends

Figure 1. IFITM1 restricts a wide range of RNA virus replication in vitro. A) Over-expression of IFITM proteins in Vero cells detected by Western blot using an antibody to the C-terminal HA tag. IFITM1 (Vero_M1), IFITM2 (Vero_M2), and IFITM3 (Vero_M3). Detection of B actin expression was used as a control, Vero Empty is the non IFITM expression vector negative control. B) Localisation of different IFITM proteins was detected by confocal microscopy using an antibody to an inserted HA tag (red) and nuclei are stained with DAPI (blue).C) Analysis of surface expression of HA tagged IFITM1 by flow cytometry on non-fixed and non-permeabilised cells. D) Co-localisation of IFITM1 (red) and wheat germ agglutinin (green) was detected by confocal microscopy. Nuclei are stained with DAPI (blue). E) Transduced Vero cells were seeded in 24 well plates and infected at a range of MOIs. Influenza A virus PR8 (H1N1 PR8), Parainfluenza virus-3 (PIV3), measles virus (rMV-Edt, rMV-EZ), Respiratory Syncytial Virus (rgRSV, RSV-B05), mumps virus (mumps), Human metapneumovirus NL/1/00-GFP (rHMPV NL1/1/00), human metapneumovirus NL/1/99-GFP (rHMPV NL/1/99), and Newcastle disease virus (rNDV). 24 hpi cells were fixed and infection level of each cell line was measured by flow cytometry. * $p<0.05$, ** $p<0.01$, *** $p<0.001$, **** $p<0.0001$ by ANOVA, when compared to cells transduced with an empty vector control (n=3).

Figure 2. IFITM1 restricts HSV-1 infection. (A) A549 cell lines stably expressing an empty vector, IFITM3, IFITM2 or IFITM1 were generated using lentiviruses. The cell lines were infected with HSV-1/GFP (MOI 5, n=3). GFP expression was measured on a Cellomics ArrayScan 7 hpi and normalized to infection levels in untransduced A549. (B) Transduced A549 cells were infected with HSV-1/GFP at an MOI of 0.01. Cells were harvested at 44 hpi and GFP expression detected by flow cytometry. (C) MRC-5 cells were treated with IFNα2a, siRNA targeting IFITM1, non-targeting siRNA or mock-treated. Total RNA was extracted and expression of IFITM1 measured. Presented as percentage expression relative to the mock treated cells +/- SD. N=3. (D) Treated MRC-5 cells were infected with HSV-1/GFP at MOI 0.5 for 7 h, GFP expression was measured on a Cellomics ArrayScan (+/- SD). Significance by ANOVA. * $p<0.05$, ** $p<0.01$, *** $p<0.001$, **** $p<0.0001$.

Figure 3. IFITM1 domains necessary for membrane localisation and virus restriction. (A) Twenty mutant human IFITM1 proteins were designed by mutating sequential blocks of six amino acids to alanine from the N to the C terminus of the protein. B) A selection of these proteins with Alanine blocks in the CIL domain were over-expressed in Vero cells using lentiviral constructs and puromycin selection; expression of the HA-tagged protein detected by Western blot. (C) Localisation of mutant protein expression was compared to wildtype human IFITM1. HA tagged proteins shown in green (anti-HA-488) and LAMP1 expression shown in red. (D) Analysis of surface expression of HA tagged CIL mutants of FITM1 by flow cytometry on non-fixed and non-permeabilsed cells (E). Representative plot showing relative surface expression of CIL mutants. (F) Vero cells were also infected with influenza, measles virus (RMV) or Mumps virus at an MOI of 1 and the level

of infection of each cell line was measured by fluorescence microscopy 24 hpi (Cellomics ArrayScan). (G) Mutant IFITM1 proteins were also over-expressed in A549 cells. Cells were infected with rgRSV (moi 0.8) for 24 hours prior to analysis of infectivity by flow cytometry. n=3. (H) 93 single nucleotide polymorphisms (SNPs) in the IFITM1 gene were identified. (I) The location of these SNPs in the human IFITM1 protein marked in red. * p<0.05, ** p<0.01, *** p<0.001, **** p<0.0001 by ANOVA, significance relative to wild-type IFITM1, n=3.

Figure 4. *Ifitm1*$^{-/-}$ mice increases RSV but not MCMV infection. Homozygous knockouts and wildtype mice were intranasally infected with 5×10^5 PFU of RSV-A2. Weight loss was measured over the course of 7 days (A). RSV viral load was measured by quantitative RT-PCR for the RSV L gene at day 4 after infection (B). Cells in Airways (C) and (D) lungs after infection. Lungs were homogenised, centrifuged and the supernatant collected for IL-6 (E) and IL-1β (F) analyses four days after infection. Mean values represent N≥5 (A-B). Points represent individual animals (C-E). WT and *Ifitm1*$^{-/-}$ mice were infected with mCMV, weight loss was measured throughout (G) and after 4 days, virus load was measured in spleen and liver by plaque assay (H). IL-6 concentrations in spleens and livers of mCMV-infected WT and *Ifitm1*$^{-/-}$ mice 4 days after infection (I). BMDMs (J) and MEFs (K) were infected with mCMV. (L) *Ifitm1* was quantified in lung, liver, and spleen of BALB/c mice (n=5). *p<0.05, **p<0.01, *** p<0.001, **** p<0.0001 by ANOVA (A, L), or t-test (B-K).

Table 1: SNPs in IFITM1 gene resulting in amino acid substitution

93 single nucleotide polymorphisms (SNPs) in the IFITM1 gene were identified from 11 UK10K disease cohorts, UK10K controls and 1000 Genomes datasets using custom scripts. 12 SNPs result in an amino acid substitution, shown in the table along with the minor allele frequencies (MAFs).

SNP ID	AA Change	Nucleotide Change	UK10K disease cohorts	UK10K controls	1000 Genomes (GMAF)
rs9667990	P13A	CCA/GCA	1	1	1
COSM46151	P14S	CCC/TCC	0.00023	-	-
rs374294080	V24M	GTG/ATG	-	-	0.00020
rs371803538	V33M	TGT/ATG	-	-	0.00020
rs764916857	F42L	TTC/TTG	-	0.00026	-
rs373112031	V61M	GTG/ATG	0.00050	-	-
rs200528039	G74R	GGG/AGG	0.00055	-	-
rs557063411	I98T	ATT/ACT	-	-	0.00020
rs201082701	V105I	GTA/ATA	-	-	0.00040
rs199539158	H113R	CAT/CGT	0.00046	0.00026	-
rs191154799	M115I	ATG/ATA	-	-	0.00040
rs572703137	Q120R	CAG/CGG	-	-	0.00020

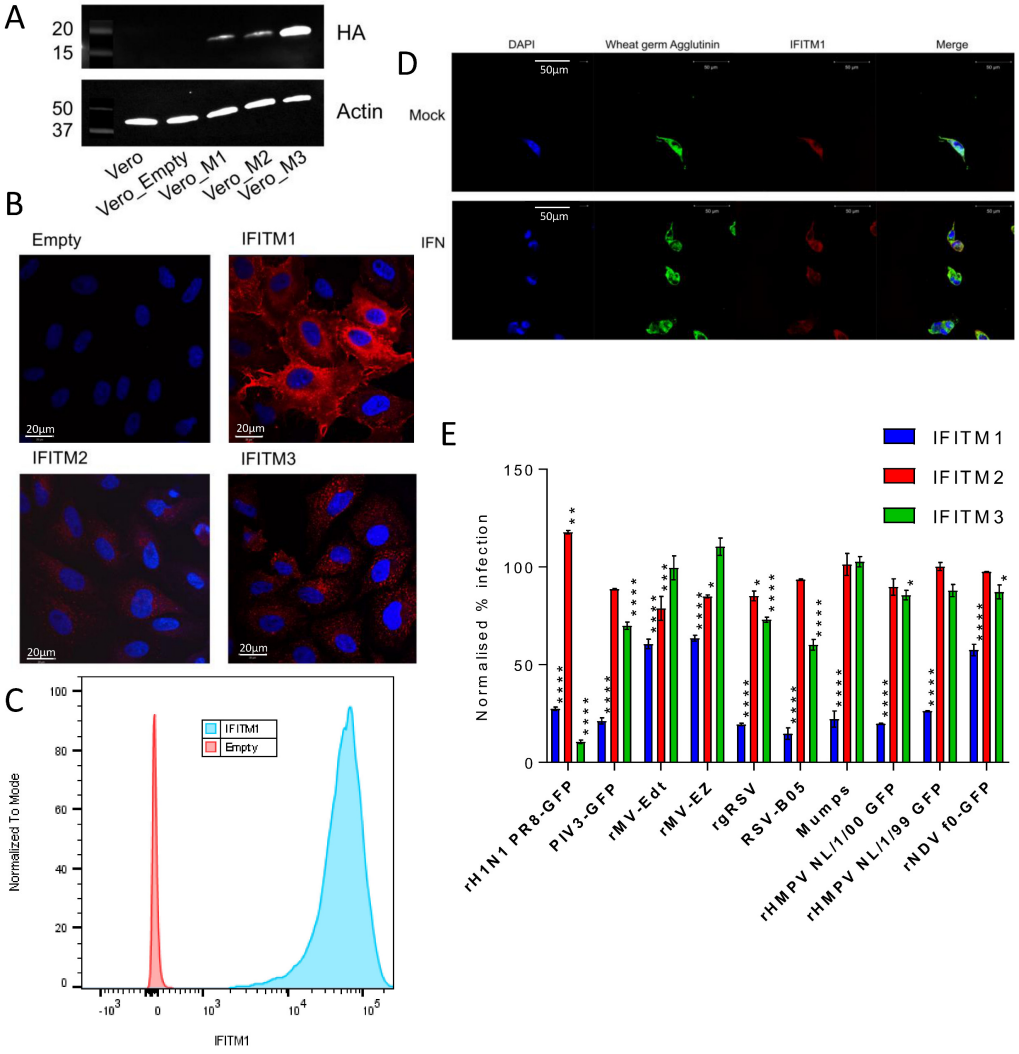

A

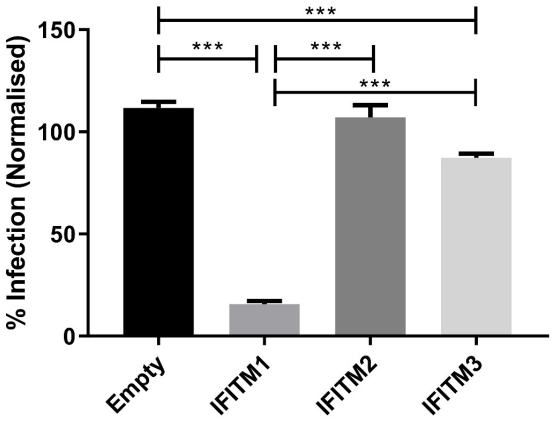

C

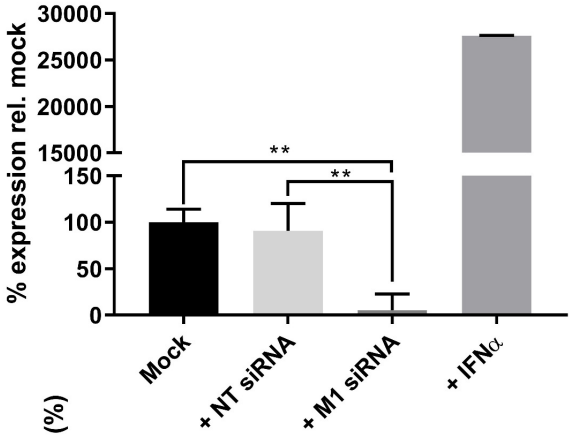

D

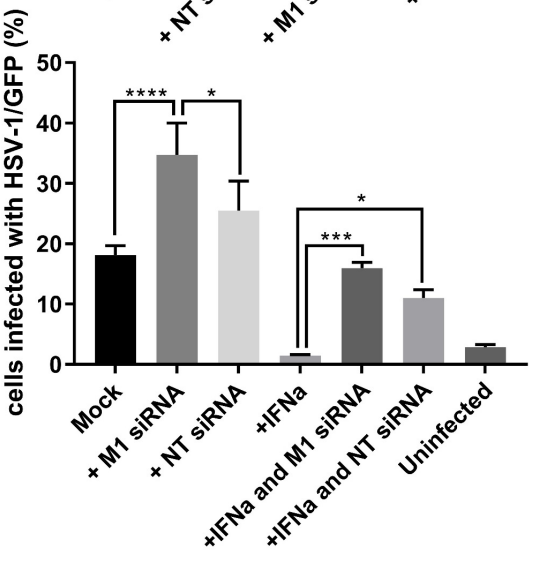

B

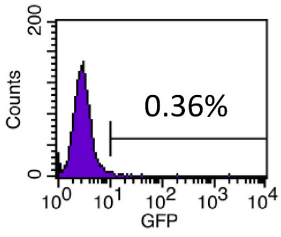

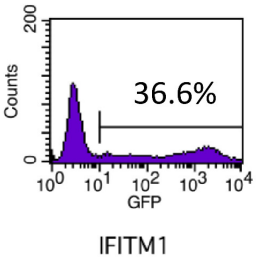

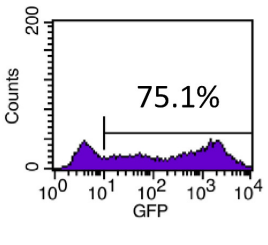

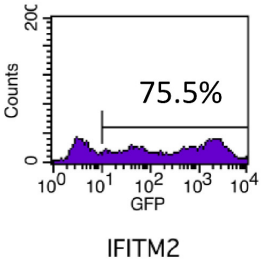

Cell Type	% of cells infected (M1)
Mock	0.36
Empty	75.06
IFITM3	58.1
IFITM2	75.5
IFITM1	36.6